ESKİŞEHİR TEKNİK ÜNİVERSİTESİ BİLİM VE TEKNOLOJİ DERGİSİ
C- YAŞAM BİLİMLERİ VE BİYOTEKNOLOJİ

Eskişehir Technical University Journal of Science and Technology
C -Life Sciences and Biotechnology

Estuscience – Life, 2026, 15 (2) pp. 130-146, DOI: 10.18036/estubtdc.1892371

RESEARCH ARTICLE

In vitro/in silico ASSESSMENT OF *Symphytum officinale* L. EXTRACT ON A549 CELLS; NEUROKININ-1 RECEPTOR-MEDIATED INTERACTIONS OF MALAXINIC ACID AND GLOBOIDNAN A

Esra TANYEL AKCIT [1], Nuket AKANIL BINGOL[2], Ece SIMSEK [3, 4*], Altinay ALTINKAYNAK[5], Gizem TUTKUN [6], Zeynep Burcu MEKIK [7], Cemilenur ATAS [8], Nilüfer IMIR [9], Ilker CINBILGEL [10,11], Kubra YILDIRIM [12,13], Emel KAYNAKCI [14, 15], Ahmet Yilmaz COBAN [16, 17]

[1] Department of Medical Services and Techniques, Dialysis Program, Vocational School of Health Services, Akdeniz University, Antalya, Türkiye.
esratanyel@akdeniz.edu.tr - 0000-0003-0561-7440

[2] Department of Biology, Arts and Science Faculty, Dumlupinar University, Kütahya, Türkiye.
nuket.abingol@dpu.edu.tr - 0000-0003-2797-3729

[3] Department of Nutrition and Dietetics, Faculty of Health Sciences, Akdeniz University, Antalya, Türkiye.
[4] Department of Medical Biotechnology, Institute of Health Sciences, Akdeniz University, Antalya, Türkiye.
ecesimsek@akdeniz.edu.tr - 0000-0002-7642-6601

[5] Department of Medical Biotechnology, Institute of Health Sciences, Akdeniz University, Antalya, Türkiye.
202350067004@ogr.akdeniz.edu.tr - 0000-0002-2012-2078

[6] Department of Medical Biotechnology, Institute of Health Sciences, Akdeniz University, Antalya, Türkiye.
202450022001@ogr.akdeniz.edu.tr - 0000-0002-6184-4974

[7] Department of Medical Biotechnology, Institute of Health Sciences, Akdeniz University, Antalya, Türkiye.
202550014001@ogr.akdeniz.edu.tr - 0009-0009-3263-911X

[8] Department of Medical Biotechnology, Institute of Health Sciences, Akdeniz University, Antalya, Türkiye.
atascemile07@gmail.com - 0000-0003-3661-1017

[9] Department of Medical Biotechnology, Institute of Health Sciences, Akdeniz University, Antalya, Türkiye.
ngimir@akdeniz.edu.tr - 0000-0002-5508-8666

[10] Department of Medical Biotechnology, Institute of Health Sciences, Akdeniz University, Antalya, Türkiye.
[11] Department of Tourism Guidance, Manavgat Tourism Faculty, Akdeniz University, Antalya, Türkiye.
icinbilgel@akdeniz.edu.tr - 0000-0003-3084-5998

[12] Department of Nutrition and Dietetics, Faculty of Health Sciences, Akdeniz University, Antalya, Türkiye.
[13] Department of Medical Biotechnology, Institute of Health Sciences, Akdeniz University, Antalya, Türkiye.
kubrayildirim@akdeniz.edu.tr - 0000-0003-0558-8619

[14] Department of Nutrition and Dietetics, Faculty of Health Sciences, Akdeniz University, Antalya, Türkiye.
[15] Department of Medical Biotechnology, Institute of Health Sciences, Akdeniz University, Antalya, Türkiye.
ekaynakci@akdeniz.edu.tr - 0000-0002-2152-0262

[16] Department of Nutrition and Dietetics, Faculty of Health Sciences, Akdeniz University, Antalya, Türkiye.
[17] Department of Medical Biotechnology, Institute of Health Sciences, Akdeniz University, Antalya, Türkiye.
cobanay2003@gmail.com - 0000-0002-8815-6063

*Corresponding Author: ecesimsek@akdeniz.edu.tr

Abstract

Lung cancer is still one of the main causes of cancer-related mortality worldwide. Angiogenesis plays a vital role in tumor progression and metastasis. Natural products have acted as valuable resources in drug discovery due to their diverse biological activities and rich content of bioactive secondary metabolites. *Symphytum officinale* L. is a medicinal plant known for its high phenolic content and has attracted research interest for various biological properties. However, its angiogenesis-related effects have not yet been clearly characterized. In this study, the phenolic content and antioxidant capacity of *S. officinale* extracts were determined, and their effects on A549 lung cancer cell proliferation were evaluated using the MTT assay. The levels of substance P, vascular endothelial growth factor, and interleukin-6 released from A549 lung carcinoma cells were quantified by ELISA. In addition, molecular docking analyses were performed to investigate the interactions of malaxinic acid and globoidnan A with receptors associated with substance P, vascular endothelial growth factor, and interleukin-6 signaling pathways. The *S. officinale* extract significantly reduced the viability and proliferation of A549 lung cancer cells. ELISA assays revealed a significant reduction ($p<0.05$) in vascular endothelial growth factor and interleukin-6 levels at early time points, whereas substance P levels did not show a consistent or statistically significant change. Molecular docking analyses suggested favorable binding interactions of malaxinic acid and globoidnan A with NK-1, NRP-1, Tie-2, and VEGFR-1 receptors. Taken together, these findings indicate that *S. officinale* extract reduces A549 cell viability and may exert transient anti-angiogenic effects on A549 cells, while its phenolic constituents exhibit strong predicted binding affinities to receptors involved in inflammatory and angiogenic signaling, particularly the NK-1 receptor.

Keywords

Symphytum officinale,
Malaxinic acid,
Globoidnan A,
Substance P,
VEGF

Time Scale of Article

Received : 18 February 2026
Accepted : 15 June 2026
Online date : 27 July 2026

1. INTRODUCTION

Natural products play an important role in drug innovation due to their broad spectrum of biological activities and the presence of bioactive secondary metabolites [1]. The genus *Symphytum* (Boraginaceae), widely distributed across Western Asia, Europe, and North America, comprises several species in Turkey. Among these, *Symphytum officinale* L. (comfrey) is one of the most widely used medicinal plants [2, 3]. Preparations derived from the aerial parts (*Symphyti herba*), leaves (*Symphyti folium*), and roots (*Symphyti radix*) have traditionally been used both externally, such as in ointments and compresses, and internally in the form of infusions and tinctures. These preparations have been used in the treatment of various conditions, including inflammatory conditions, tonsillitis, and respiratory disorders [4-6].

Symphytum genus are known to contain diverse secondary metabolites, including naphthoquinones, flavonoids, terpenoids, and phenolic derivatives. Phytochemical investigations of this genus have led to the isolation and characterization of numerous compounds, such as phenolic acids, flavonoids, aliphatic ketones, naphthazarins, and naphthoquinones. Among these, caffeic acid, globoidnan A, globoidnan B, rabdosiin, malaxinic acid, and rosmarinic acid have been reported as major phenolic constituents of *S. officinale*. In addition, Boraginaceae family are known to contain pyrrolizidine alkaloids, which should be considered in terms of safety [6-8]. These phytochemical constituents have been reported to exhibit antioxidant, antitumor, and anti-inflammatory activities [9].

Lung cancer accounts for a significant proportion of malignant tumors worldwide. Non-small cell lung cancer (NSCLC), which represents approximately 85–90% of all cases, is associated with high morbidity and mortality [10]. Angiogenesis plays a central role in lung cancer progression by promoting tumor growth, invasion, metastasis, and modulation of the tumor microenvironment. The increasing development of resistance to conventional chemotherapy has highlighted the need for alternative therapeutic strategies, including approaches targeting angiogenesis. Among angiogenic mediators, the vascular endothelial growth factor (VEGF) family represents the primary target of anti-angiogenic therapies. In addition, interleukin-6 (IL-6), a pro-inflammatory cytokine that interacts with VEGF and other signaling molecules, has been shown to enhance angiogenic responses [11]. Substance P (SP), a neuropeptide involved in

inflammatory signaling, has also been reported to promote angiogenesis and to increase tumor cell invasion and metastasis within the lung tumor microenvironment [12]. Although studies have reported various biological effects of *S. officinale* extracts and their bioactive constituents, the effects of this plant extract and its phenolic components on angiogenesis-related factors released from cancer cells, as well as their potential interactions with angiogenic receptor proteins, remain largely unexplored.

The total phenolic content and antioxidant capacity of *S. officinale* were determined at the Food Safety and Agricultural Research Center of Akdeniz University. The effects of *S. officinale* extract on the proliferation of A549 lung cancer cells were evaluated. To explore the potential involvement of inflammatory and angiogenic pathways, the levels of SP, VEGF, and IL-6 were evaluated following treatment. In addition, molecular docking analyses were performed to investigate the potential interactions of malaxinic acid and globoidnan A, phenolic constituents of *S. officinale*, with angiogenesis-related receptors, including neurokinin-1 (NK-1), vascular endothelial growth factor receptor 1 (VEGFR-1), neuropilin-1 (NRP1), and Tie2.

2. MATERIALS AND METHODS

2.1. Plant Material and Extraction

Plant extract (10 g/25 ml water) was given as a kind gift from Kütahya Dumlupınar University, Hekim Sinan Medical and Aromatic Plants Research Center. In this study, 10 g of the plant's leaves were extracted using 25 mL of water.

2.2. Determination of Total Phenolic and Total Antioxidant Capacity of Plant Extract

The total phenolic and total antioxidant capacity of plant extract was determined by Akdeniz University, Food Safety and Agricultural Research Center with a report number 2023-355.

2.3. Cell Culture Conditions

A549 cells (ATCC®CCL-185 ™) were cultured in DMEM (Gibco, Carlsbad, CA, USA) containing 10% fetal bovine serum (FBS), 10 µg/mL gentamicin, and 5% sodium pyruvate. The cells were incubated under 5% CO_2 with 95% humidity at 37°C.

2.4. EC_{50} Analysis, and Cell Viability

The MTT [3-(4,5-dimethylthiazol-2-yl)-2,5-diphenyltetrazolium bromide] assay was used to evaluate cell viability following treatment with the plant extract. The cells were seeded into 96-well plates at a density of 5×10^3 cells per well in 200 µL of culture medium and allowed to attach overnight. A stock solution of the plant extract (100 mg/mL) was serially diluted to obtain final concentrations of 1.87, 3.75, 12.5, 25, 50 and 100 µg/mL. Cells were treated with the extract and incubated for 24, 48, or 72 hours at 37°C in a humidified atmosphere containing 5% CO_2.

At the end of each incubation period, the culture medium was removed, and 90 µL of serum-free medium together with 10 µL of MTT reagent was added to each well. Following a 4-hour incubation, the MTT-containing medium was carefully removed, and 100 µL of dimethyl sulfoxide (DMSO) was added to each well to dissolve the formazan crystals. The plates were gently shaken for 10 minutes in the dark, and absorbance was measured at 570 nm using a microplate reader.

Cell viability was calculated as a percentage relative to untreated control cells (0 mg/mL) according to the formula:

$$Viability\ \% = \frac{Absorbance\ of\ treated\ cells}{Absorbance\ of\ control\ cells} \times 100$$

2.5. ELISA Assays for SP, VEGF, and IL-6

Cells were seeded at a density of 1×10^6 cells per well in 2 mL of complete culture medium in 6-well plates. After overnight attachment, cells were treated with *S. officinale* extract at two different concentrations (1 and 2 mg/mL). The levels of SP, VEGF, and IL-6 released into the culture supernatant were quantified using enzyme-linked immunosorbent assay (ELISA) kits according to the manufacturer's instructions (Invitrogen Corp., Camarillo, CA, USA) after 24 and 48 hours of treatment. Recombinant human SP, VEGF, and IL-6 standards provided with the kits were serially diluted to generate standard curves. Results obtained from treated samples were compared with those of untreated control cells. All experiments were performed in four independent replicates, and data are presented as mean ± standard error (SE).

2.6. *In Silico* Studies

2.6.1. Protein structure preparation

X-ray crystal structures were obtained from the Protein Data Bank (PDB). PDB file names are as follows: Human neurokinin-1 receptor, PDB ID: 6e59; Human vascular endothelial growth factor receptor-1, PDB ID: 1vr2; human Neuropilin-1 receptor, PDB ID: 1kex; and tyrosine kinase receptor, PDB ID: 1fvr. BIOVIA Discovery Studio was used for Protein Preparation.

2.6.2. Ligand structure preparation

3-D Structures of Malaxinic acid and Globoidnan A were obtained from PubChem. PubChem IDs of Malaxinic acid and Globoidnan A were 162641407 and 135263380 respectively. Conjugate Gradients and OpenBabel software in the PyRx program were used for energy minimization as an MMFF94 force field and optimization algorithm [13].

2.6.3. Molecular docking studies

CB-Dock-2 uses efficient quasi-Newton and Broyden-Fletcher-Goldfarb-Shanno methods for local optimization. Ligands were docked to the binding site cavity by the automated system in the program. Docking calculations were performed with an exhaustiveness option of 9 (average accuracy). The Vina gives docking scores as predicted inhibition constants (Ki), which is derived from Gibbs free energy of binding calculated by the following equations:

$G = -(\ln Ki)$ (1)

$Ki = e^{-\Delta GRT}$

where R (gas constant) is 1.98 cal/mol K, and T is 98.15 K. The BIOVIA Discovery Studio program was used to visualize the results.

2.7. Statistical Analysis

Cell viability was assessed based on the absorbance values obtained after the cells were treated with the drug. These values were normalized to the control group (0 μg/mL), and the percentage of viable cells was calculated. Bar graphs showed the were used to present the reduction in A549 cell viability, and the data were presented as the mean ± SD. Statistical differences between groups were evaluated using one-way ANOVA and the Dunnett's multiple comparison test with GraphPad Prism 8.0.2 software (GraphPad Software, San Diego, USA).

The half-maximal effective concentration (EC_{50}) of the extract and the EC_{50} values for 24, 48, and 72 hours were determined by plotting dose-response curves using non-linear regression. p-value of < 0.05 was considered statistically significant.

3. RESULTS

3.1. *In vitro* Studies

3.1.1. EC_{50} analysis

As shown in Figure 1, cells treated with *S. officinale* extract at concentrations differing from 1.87 to 100 µg/mL exhibited a decrease in viability compared with the control group. However, at 24 and 48 h, the response didn't reach the threshold required to reliably calculate an EC_{50} value. In contrast, after 72 h of exposure, a biologically meaningful EC_{50} of approximately 40 µg/mL was observed ($p < 0.05$), suggesting a response that varies as a function of both exposure time and concentration.

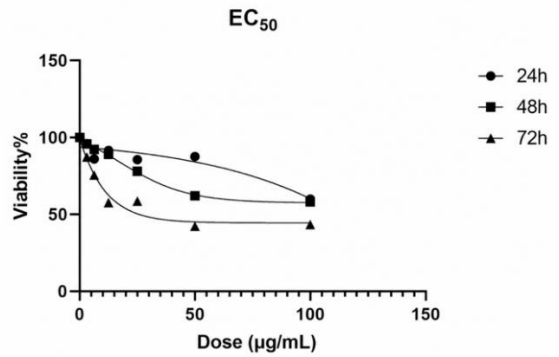


Figure 1. Dose-response curves and EC_{50} values for plant extract treatment at 24, 48, and 72 hours.

3.1.2. Cell viability

The effect of *S. officinale* plant extract (1.87-100 µg/mL) on the viability of A549 human lung carcinoma cells was assessed over 24, 48, and 72 h using the MTT assay, which measures mitochondrial activity as an indicator of metabolic function and cell survival. Cell viability was expressed as a percentage relative to untreated control cells. A dose-dependent decrease in cell viability was observed at higher concentrations across all incubation periods. At 24 h, *S. officinale* treatment demonstrated a concentration-dependent reduction in viability, with a statistically significant effect detected only at the highest dose (100 µg/mL), where viability declined to $59.88 \pm 4.53\%$ relative to control ($p < 0.001$). No significant change was observed at 1.87 µg/mL ($p = 0.1068$). After 48 h, statistically significant decreases in cell viability were observed at concentrations ≥12.5 µg/mL, with the strongest effect at 100 µg/mL, where viability decreased to $57.97 \pm 4.18\%$ ($p < 0.0001$). Similarly, at 72 h, *S. officinale* treatment was associated with a concentration-dependent reduction in A549 cell viability, with significant decreases at ≥12.5 µg/mL. The maximal effect was observed at 100 µg/mL, where viability declined to $41.27 \pm 5.88\%$ relative to control ($p < 0.0001$). Together, these data suggest that *S. officinale* progressively impairs A549 cell viability in a manner dependent on both exposure duration and concentration.

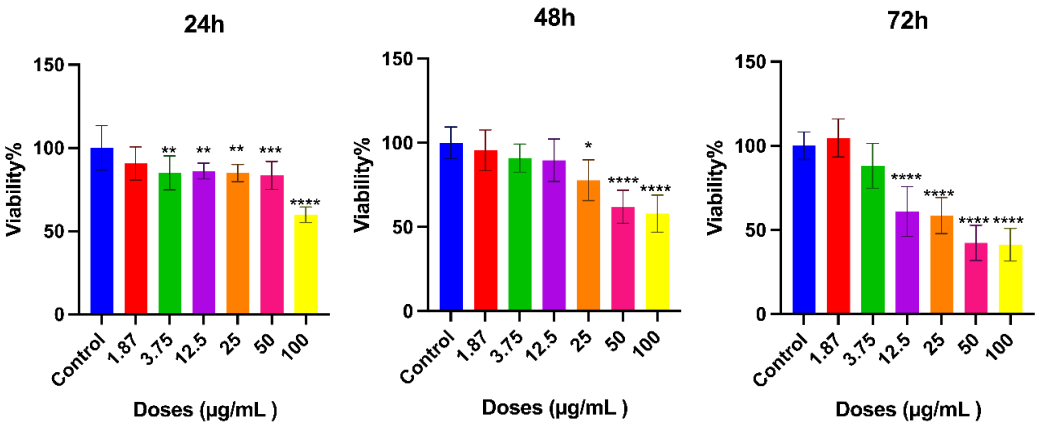


Figure 2. Concentration- and time-dependent effects of *S. officinale* extract treatment on A549 human lung carcinoma cell viability. The results are presented as the percentage change in viability relative to the control group and expressed as mean ± standard deviation (SD).

3.2. The Amount of SP Released from A549 Cells

The levels of SP released from A549 human lung carcinoma cells following treatment with 1 mg/mL and 2 mg/mL extract concentration doses of *S. officinale* extract were quantified at 24- and 48-hours using ELISA method. Untreated wells served as negative controls. After 24 hours, a slight increase in SP levels was observed in both treatment groups compared to the control group. Conversely, at the end of the 48-hour incubation period, a minimal decrease in SP levels was observed. Overall, there was no significant increase or decrease (Figure 3).

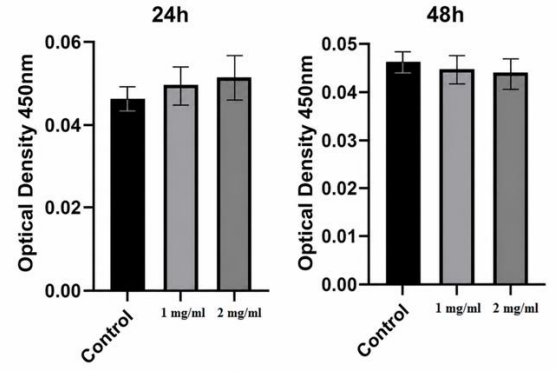


Figure 3. Quantification of SP levels released from A549 human lung carcinoma cells following treatment with *S. officinale* extract at 24 and 48 hours respectively. The results represent the mean standard deviation (SD).

3.3. The Amount of VEGF Released from A549 Cells

To evaluate the effect of *S. officinale* extract on angiogenic signaling, VEGF levels were measured in A549 lung carcinoma cell culture supernatants after 24 and 48 hours of treatment with ELISA methods. Two extract concentrations 1 mg/mL and 2 mg/mL were applied, and untreated wells served as controls. After 24 hours, both extract concentrations had dose-dependent decreased VEGF levels, but the 2 mg/ml concentration was found to be statistically significant compared to the control group. In contrast, after 48 hours of treatment, VEGF levels rebounded, showing no significant difference from control values. This may indicates that the anti-angiogenic effect of *S. officinale* extract is likely short-term and not sustained over extended exposure periods.

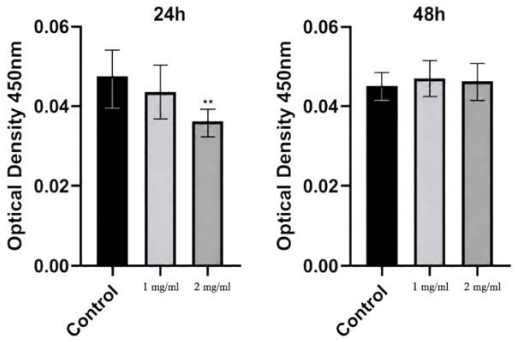


Figure 4. Quantification of VEGF levels released from A549 human lung carcinoma cells following treatment with *S. officinale* extract at 24 and 48 hours respectively. The results represent the mean ± standard deviation (SD).

3.4. The Amount of IL-6 Released from A549 Cells

The impact of *S. officinale* extract on IL-6 secretion by A549 human lung carcinoma cells was assessed after 24 and 48 hours of treatment. Cells were exposed to concentrations of 1 mg/mL and 2 mg/mL of the extract, and untreated cells served as controls. After 24 hours of treatment, no significant change in IL-6 levels was observed in either of the extract-treated groups compared to controls. However, at 48 hours, a time- and dose-dependent modulation of IL-6 secretion became apparent. Specifically, IL-6 levels were decreased at the 1 mg/mL dose relative to control, while a notable increase was observed at the 2 mg/mL dose. These findings suggest that *S. officinale* extract may exert a biphasic immunomodulatory effect on IL-6 release in A549 cells over prolonged exposure periods.

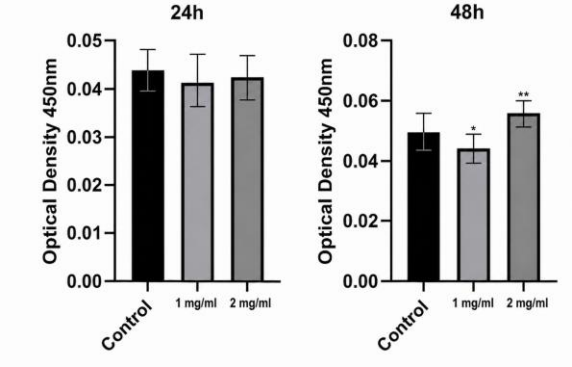


Figure 5. Quantification of IL-6 levels released from A549 human lung carcinoma cells following treatment with *S. officinale* extract at 24 and 48 hours respectively. The results represent the mean ± standard deviation (SD).

3.5. The Total Phenolic and Total Antioxidant Capacity of Plant Extract

The total phenolic and total antioxidant capacity of plant extract was determined as 84.57 mg Gallic acid equivalent /100 mL and 105.97 mg Trolox acid equivalent /100 mL, respectively.

3.6. *In silico* Results

Molecular docking simulations were performed to investigate the interactions between two phenolic compounds isolated from *S. officinale*, malaxinic acid and globoidnan A, and key receptor proteins involved in inflammation and angiogenesis. A clearer comparison of the *in silico* molecular docking data was achieved by presenting the binding profiles of malaxinic acid and Globoidnan A in two separate tables (Table 1 and Table 2). Each table presents the interacting target receptors, PDB IDs, number of

amino acid residues involved, key binding residues, and binding affinity. This structured presentation supports a better interpretation of the compounds predicted interactions with receptors implicated in angiogenic and inflammatory pathways.

Table 1. Molecular Docking Results: Malaxinic Acid

Ligand	Target Receptor	PDB ID	Number of Interacting Residues	Key Residues	Binding Affinity (kcal/mol)
Malaxinic acid	NK-1	6e59	19	THR86, PHE90, HIS108, ASN109, ILE113, TRP261	-8.5
	NRP-1	1kex	19	VAL90, SER91, ASP96, THR99, ARG130	-6.3
	Tie2	1fvr	17	LYS1059, CYS1063, ASP1065, TYR1102, PHE1111	-7.3
	VEGFR-1	1vr2	18	LEU840, VAL848, GLU917, LYS920, ASN923, ASP1046	-6.9

Malaxinic acid exhibited strong binding affinities with several targets. Among the four receptors, malaxinic acid showed the highest binding affinity to the NK-1 receptor.

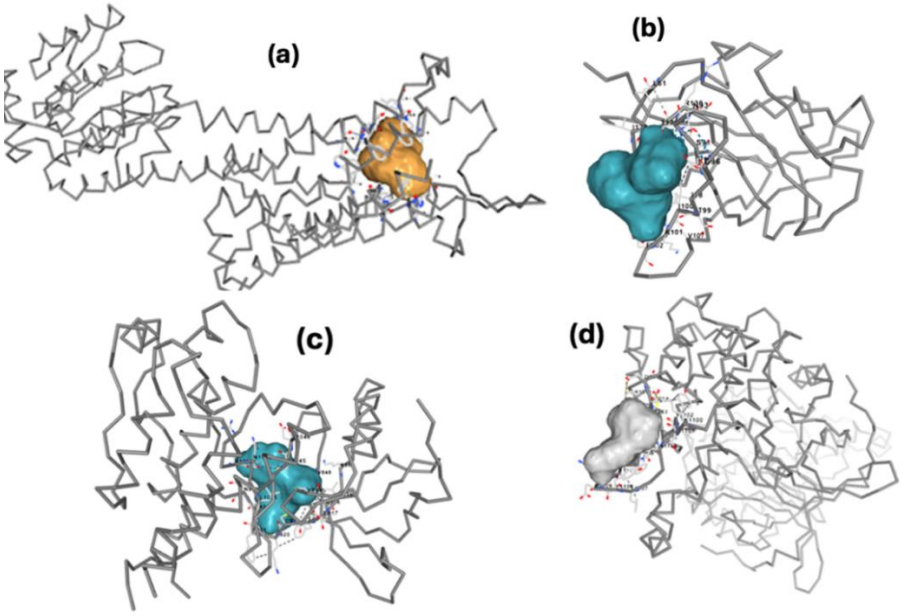


Figure 6. (a) Molecular docking interactions between malaxinic acid and the NK-1 (PDB ID: 6e59). **(b)** Molecular docking interactions between malaxinic acid and the human NRP-1 (PDB ID: 1kex). **(c)** Molecular docking interactions between malaxinic acid and Tie2 (PDB ID: 1fvr). **(d)** Molecular docking interactions between malaxinic acid and the VEGFR-1 (PDB ID: 1vr2).

SP inhibits cancer cells through the NK-1 receptor. Figure 6 illustrates the predicted binding interactions between malaxinic acid, a phenolic compound derived from *S. officinale*, and the active site of NK-1 receptor using molecular docking simulations. Malaxinic acid interacted with 19 active site amino acids of NK-1 namely THR86, PHE90, HIS108, ASN109, PRO112, ILE113, VAL116, GLN165, TYR196, HIS197, ILE198, VAL200, THR201, ILE204, TRP261, PHE264, HIS265, PHE268 and LEU269. These interactions suggest multiple binding modes: hydrogen bonding likely occurs with polar residues like THR86, HIS108, and ASN109; aromatic π–π stacking interactions are plausible between the aromatic rings of malaxinic acid and aromatic residues such as PHE90 and TRP261; and hydrophobic interactions may be established with non-polar residues such as ILE113. Consequently, the *in silico* binding energies point to a potentially stable interaction with the NK-1 receptor, which may underlie the compound's capacity to influence receptor-mediated signaling.

VEGF promotes tumor angiogenesis through its interaction with NRP-1, a co-receptor involved in angiogenic signaling. Therefore, NRP-1 has become a promising target in cancer therapy research. Figure 7 illustrates the binding interactions between malaxinic acid, a phenolic compound derived from *S. officinale*, and the NRP-1 receptor. Malaxinic acid interacted with 19 active site amino acids of NRP-1, namely LEU61, VAL90, SER91, SER92, ASN93, ASP96, ILE98, THR99, ILE100, LYS101, GLU102, VAL107, PRO124, LYS125, PRO126, LEU127, ILE128, THR129 and ARG130. Hydrogen bonding is likely formed with polar residues such as SER91, ASP96, and THR99, stabilizing the complex via polar contacts. Electrostatic interactions may also occur between the negatively charged groups of the ligand and the positively charged ARG130 side chain. Additionally, hydrophobic contacts with nonpolar residues like VAL90 may further enhance binding affinity. Accordingly, the favorable *in silico* binding profile of malaxinic acid with NRP-1 suggests that it may have the potential to modulate angiogenic signaling pathways associated with cancer progression.

The predicted binding interactions between malaxinic acid and Tie2, a key receptor involved in angiogenesis and vascular homeostasis. Malaxinic acid interacted with 17 active site amino acids of Tie-2 namely LYS1059, PRO1060, LEU1061, ASN1062, CYS1063, ASP1064, ASP1065, LYS1100, THR1101, TYR1102, ASN1104, LEU1107, TYR1108, GLU1109, LYS1110, PHE1111 and THR1112. These findings suggest several potential binding modes. Hydrogen bonds are likely formed with polar or charged residues such as ASP1065 and CYS1063, contributing to the specificity and orientation of the ligand. The presence of LYS1059, a positively charged residue, indicates possible electrostatic interactions with acidic groups of malaxinic acid. Furthermore, aromatic interactions such as π–π stacking with TYR1102 and PHE1111 may enhance binding affinity and stability. Overall, these interactions indicate a favorable binding profile, suggesting that malaxinic acid may influence angiogenesis through modulation of Tie2 receptor activity.

Figure 6d presents the molecular docking results illustrating the interaction between malaxinic acid and VEGFR-1, a key receptor involved in the regulation of angiogenesis. Malaxinic acid interacted with 18 active site amino acids of VEGF-1 namely LEU840, VAL848, ALA866, LYS868, VAL899, VAL916, GLU917, PHE918, CYS919, LYS920, PHE921, GLY922, ASN923, ARG1032, ASN1033, LEU1035, VYS1045 and ASP1046. These interactions suggest a combination of binding modes. Hydrogen bonding may occur through polar and charged residues such as GLU917, ASN923, and ASP1046, which helps stabilize the ligand in the binding pocket. Electrostatic interactions are likely between the negatively charged groups of malaxinic acid and the positively charged LYS920. Additionally, hydrophobic interactions with nonpolar residues such as LEU840 and VAL848 further contribute to the stability of the ligand–receptor complex. Collectively, these diverse molecular interactions highlight a favorable binding affinity, suggesting that malaxinic acid may inhibit VEGFR-1 signaling and thereby exert anti-angiogenic effects.

Globoidnan A also demonstrated notable receptor binding properties. Among the four receptors, globoidnan A has shown the highest affinity to the NK-1 receptor, like malaxinic acid.

Table 2. Molecular Docking Results: Globoidnan A

Ligand	Target Receptor	PDB ID	Number of Interacting Residues	Key Residues	Binding Affinity (cal/mol)
Globoidnan A	NK-1	6e59	21	PHE90, ASN109, VAL116, TYR196, HIS197, TRP261, PHE264, TYR272	-9.7
	NRP-1	1kex	18	VAL90, SER92, ASP96, ILE98, LYS101, GLU102, AERG130	-7.8
	Tie2	1fvr	16	LYS1059, ASP1064, TYR1102, GLU1109, PHE1111	-7.2
	VEGFR-1	1vr2	21	PRO839, LEU840, VAL848, GLU917, PHE918, ASN923, ASP1046, PHE1047	-8.4

Globoidnan A formed strong interactions with 21 residues at the NK-1 receptor, implying a high potential to modulate inflammation and tumor progression (Figure 7a). For the NRP-1 receptor, globoidnan A formed stable interactions with 18 residues, albeit suggesting a slightly weaker modulation compared to malaxinic acid (Figure 7b). Docking with the Tie2 receptor showed 16 key interactions, indicating the capacity to influence vascular pathways (Figure 7c). Lastly, globoidnan A exhibited strong and stable binding to VEGFR-1, interacting with 21 amino acid residues, reinforcing its potential to inhibit angiogenesis (Figure 7d).

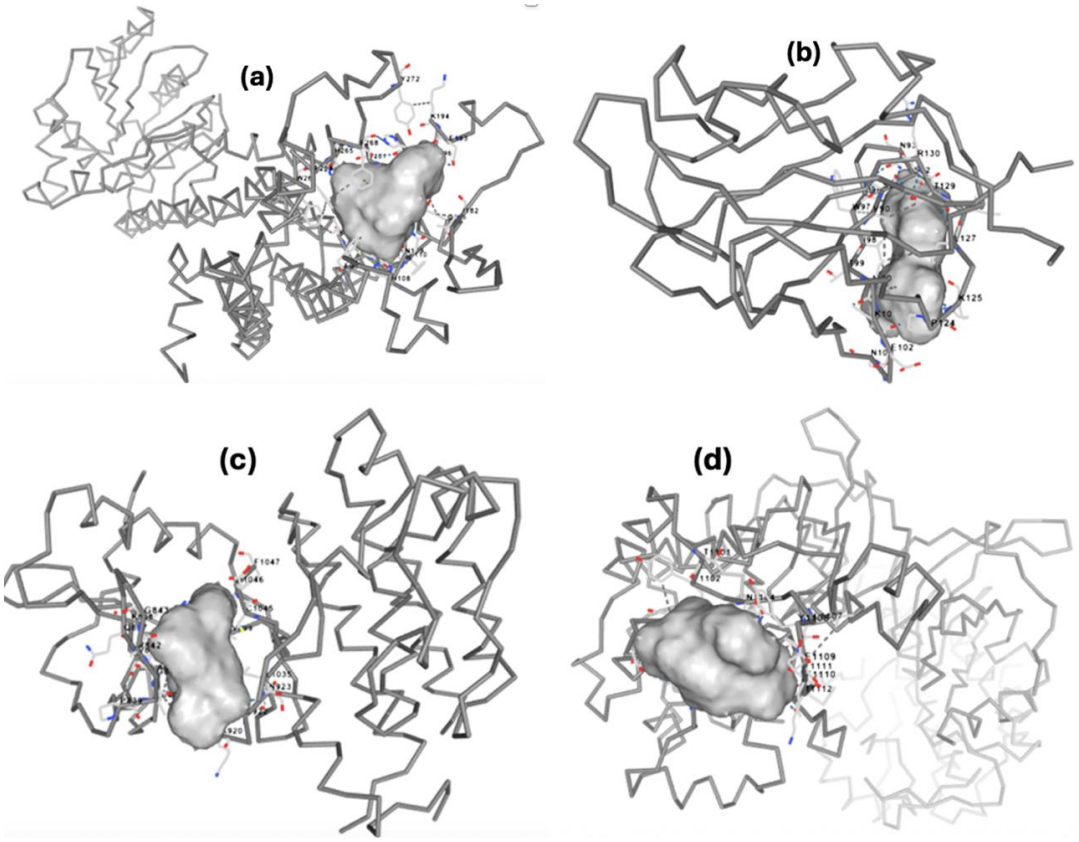


Figure 7. (a) Molecular docking interactions between globoidnan A and the NK-1 (PDB ID: 6e59). **(b)** Molecular docking interactions between globoidnan A and the NRP-1 (PDB ID: 1kex). **(c)** Molecular docking interactions between globoidnan A and the Tie2 (PDB ID: 1fvr). **(d)** Molecular docking interactions between globoidnan A and the VEGFR-1 (PDB ID: 1vr2).

Figure 7a illustrates the molecular docking results, showing the interaction of globoidnan with the NK-1 receptor, a G-protein-coupled receptor involved in inflammation, pain signaling, and cancer cell proliferation. Globoidnan A interacted with 21 active site amino acids of NK-1 namely PHE90, HIS108, ASN109, PHE110, PRO112, ILE113, VAL116, GLN165, ILE182, GLU193, LYS194, TYR196, HIS197, VAL200, THR201, ILE204, TRP261, PHE264, HIS265, PHE268 and TYR272. The binding interaction of the globoidnan A with the NK-1 is shown in Fig. 10. The binding profile suggests multiple interaction types contributing to a high binding affinity. Hydrogen bonds may be formed with polar residues such as ASN109 and HIS197, aiding in ligand stabilization. Aromatic residues including PHE90, TYR196, TRP261, PHE264, and TYR272 are likely to engage in π–π stacking interactions with the aromatic rings of globoidnan A. Additionally, hydrophobic interactions involving residues like VAL116 may further reinforce the binding. The predicted binding interactions suggest that globoidnan A may engage the NK-1 receptor and could potentially influence neuropeptide-mediated pathways involved in inflammation and tumor progression.

Figure 7b presents the molecular docking results of globoidnan A with the NRP-1 receptor, a co-receptor known to enhance VEGF signaling and facilitate tumor angiogenesis. Molecular docking analysis showed that globoidnan A interacts with 18 amino acid residues within the binding pocket of the NRP-1 receptor (PDB ID: 1kex). Key interacting residues include VAL90, SER92, ASP96, ILE98, LYS101, GLU102, and ARG130. These interactions suggest a combination of binding modes. Hydrogen bonding is likely between globoidnan A and polar residues such as SER92 and ASP96, while electrostatic interactions may occur between negatively charged functional groups of the ligand and the positively charged side chains of LYS101 and ARG130. Additionally, hydrophobic interactions with residues like

VAL90 and ILE98 could further stabilize the ligand within the receptor cavity. Although these interactions indicate a comparatively moderate binding affinity relative to NK-1, they suggest that the compound may modulate VEGF-related signaling via NRP-1

Figure 7c demonstrates the predicted binding interactions between globoidnan A and the Tie2 receptor, a tyrosine kinase involved in vascular development, endothelial cell survival, and angiogenesis. Molecular docking simulations revealed that globoidnan A interacts with 16 amino acid residues within the binding site of the Tie2 receptor (PDB ID: 1fvr), namely LYS1059, PRO1060, LEU1061, ASN1062, CYS1063, ASP1064, ASP1065, THR1101, TYR1102, ASN1104, LEU1107, TYR1108, GLU1109, LYS1110, PHE1111 and THR1112. These interactions suggest multiple binding modes. Hydrogen bonds may be formed with polar or charged residues such as ASP1064 and GLU1109, facilitating stable ligand orientation. The presence of LYS1059, a basic residue, suggests potential electrostatic interactions with acidic groups on the ligand. Additionally, aromatic interactions like π–π stacking between the aromatic rings of globoidnan A and residues such as TYR1102 and PHE1111 may enhance binding affinity. These combined binding modes support the hypothesis that globoidnan A may influence Tie2-mediated angiogenic signaling pathways relevant to tumor biology and inflammation.

Figure 7d presents the predicted molecular interactions between globoidnan A and VEGFR-1, a receptor tyrosine kinase involved in mediating angiogenesis and vascular permeability in cancer progression. Molecular docking analysis revealed that globoidnan A forms interactions with 21 amino acid residues within the binding site of the VEGFR-1 namely PRO839, LEU840, GLY841, ARG842, GLY843, GLN847, VAL848, ALA866, LYS868, VAL899, VAL916, GLU917, PHE918, CYS919, LYS920, GLY922, ASN923, LEU1035, CYS1045, ASP1046 and PHE1047. These residues suggest the presence of diverse binding interactions. Hydrogen bonds may occur with polar residues such as ASN923 and ASP1046, helping to anchor the ligand within the binding cavity. Electrostatic interactions are possible between the negatively charged GLU917 and acidic ligand moieties, while aromatic stacking may occur with residues like PHE918 and PHE1047, enhancing binding strength. Additionally, hydrophobic contacts with PRO839, LEU840, and VAL848 contribute to the overall stability of the complex. Collectively, these interactions support the hypothesis that globoidnan A has a high binding affinity for VEGFR-1 and may effectively modulate VEGF-mediated angiogenic signaling in tumor biology.

These molecular docking results suggest that both malaxinic acid and globoidnan A possess significant binding affinities toward multiple cancer- and inflammation-related targets, supporting the experimental observations of anti-inflammatory and anti-angiogenic effects of *S. officinale* extract (Figure 8).

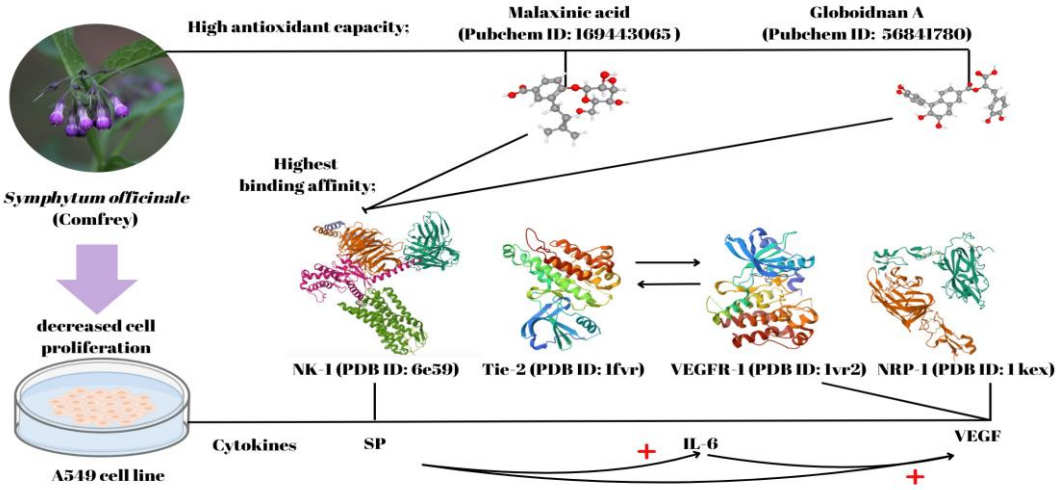


Figure 8. Illustration of the proposed mechanism by which *S. officinale* compounds (malaxinic acid and globoindnan A) may reduce A549 cell proliferation. These compounds show strong binding to NK-1, Tie-2, VEGFR-1, and NRP-1, key receptors in the SP–IL-6–VEGF inflammatory and angiogenic axis.

4. DISCUSSION

Medicinal plants have gained attention as potential sources of anticancer agents due to their bioactive compounds, which often exhibit selective antiproliferative activity against tumor cells while sparing normal tissues. Among them, *S. officinale* is a traditional medicinal plant historically used for inflammation reduction. Recent studies have expanded its known properties, highlighting its significant wound-healing, antioxidant, anti-inflammatory, and cytostatic activities [14,15]. Phytochemical analyses of *S. officinale* extracts have identified high concentrations of phenolic compounds, such as rosmarinic acid, caffeic acid, and chlorogenic acid, which contribute to its strong biological activities [16]. Concentrated extracts have demonstrated notable cytostatic effects against HeLa cancer cell line [17]. In addition, *S. officinale* has been reported to exert anticancer effects by inhibiting growth factor–related signaling pathways, including IGF-II, in hepatocellular carcinoma models [18]. Taken together, its rich phytochemical composition and promising biological activities position *S. officinale* as an attractive candidate for further exploration in cancer therapy.

Building on this evidence, the present study evaluated the *in vitro* and *in silico* effect of *S. officinale* on A549 human lung carcinoma cells. For the first time, the potential modulation of inflammation- and angiogenesis-related markers, including SP, VEGF, and IL-6, was examined at both the cellular and molecular levels. The present study demonstrates that *S. officinale* extract induces a time-dependent reduction in A549 cell viability, as reflected by the progressive shift in EC_{50} values over time. These findings are consistent with previous reports showing a significant (~57.6%) mitotic inhibitory effect of *S. officinale* on HeLa cells [17]. Although the extract displayed clear anticancer potential, the molecular mechanisms underlying these effects required further investigation. Accordingly, SP, IL-6, and VEGF levels were quantified by ELISA, and the two most abundant bioactive compounds in the extract were subjected to *in silico* analyses to explore their associations with angiogenesis and pain related signaling pathways. In parallel, the antioxidant capacity of the extract was assessed. Consistent with its high phenolic content, *S. officinale* extract demonstrated marked antioxidant activity, in agreement with previous studies employing DPPH, FRAP, and total phenolic content analyses, which reported particularly strong antioxidant effects in ethanol/water extracts [19]. Earlier work has also shown that *S. officinale* exhibiting minimal cytotoxicity toward normal human skin fibroblasts, even at concentrations up to 200 µg/mL [16,17].

SP is a neuropeptide known to play a role in tumor progression, angiogenesis, and inflammation [20,21]. In the present study, treatment of A549 cells with *S. officinale* extract for 24 and 48 hours did not result in statistically significant alterations in SP levels, despite previous reports demonstrating measurable SP release within 24-48 hours following stimulation in other cellular models [22,23]. Nonetheless, molecular docking analyses indicated that malaxinic acid and globoidnan A exhibit strong predicted binding affinities toward the NK-1 receptor. Among the three receptors examined, both compounds showed the highest predicted affinity for NK-1. Given the absence of statistically significant alterations in SP levels, the predicted NK-1 receptor interactions of malaxinic acid and globoidnan A are more likely to reflect SP-independent modulation of NK-1 associated signaling pathways. In this context, further studies should molecular dynamics simulations and functional assays are warranted to clarify the biological relevance of these interactions. While docking provides a rapid and cost-effective approach for screening ligand receptor interactions [24], its reliance on static protein structures limits its ability to capture protein flexibility, solvent effects, and entropic contributions to binding [25,26]. *S. officinale* and its bioactive constituents, particularly rosmarinic acid, can modulate cytokine production in immune cells, leading to reduced secretion of inflammatory mediators such as IL-6 [6]. Green silver nanoparticles synthesized from *S. officinale* extracts have been shown to suppress IL-6 production in UVB-irradiated HaCaT cells, further suggesting that the extract may influence inflammatory signaling [27]. In the present study, changes in IL-6 secretion were inconsistent across time points, representing a limitation that warrants further investigation.

Notably, the reduction in VEGF levels observed at 24 hours suggests a potential short-term modulation of angiogenesis-related markers of *S. officinale* extract. This observation aligns with previous reports indicating that plant-derived compounds can suppress VEGF production and thereby limit tumor-associated angiogenesis [18]. The attenuation of this effect at later time points may reflect degradation of bioactive compounds under culture conditions or the activation of compensatory angiogenic pathways within cancer cells, as reported for other botanical extracts [28]. The inhibition of VEGF signaling by natural compounds is frequently associated with suppression of regulatory pathways such as IGF-II and NF-κB, which are also implicated in the anticancer activity of *S. officinale* [29]. Collectively, these findings suggest that *S. officinale* extract exhibits a promising but transient anti-angiogenic effect *in vitro*, highlighting the importance of formulation stabilization for sustained activity. The anticancer, anti-inflammatory, and antioxidant effects of *S. officinale* are largely attributed to its polyphenolic constituents, including rosmarinic, chlorogenic, and caffeic acids [2]. In this study, malaxinic acid and globoidnan A were investigated for their potential interactions with apoptosis and angiogenesis related receptors *in silico*. Malaxinic acid demonstrated strong predicted binding affinities toward all tested receptors and formed interactions with key active-site residues, suggesting a potential to modulate receptor function. Its interactions with NRP-1 and VEGFR-1 support a possible anti-angiogenic role by interfering with VEGF-mediated signaling and tumor vascularization [28]. Globoidnan A exhibited comparatively lower affinity for NRP-1 but showed strong binding to NK-1 and VEGFR-1, indicating a potential capacity to suppress VEGF-driven angiogenic pathways. Both compounds also interacted with the Tie2 receptor, which plays a central role in vascular stability and tumor neovascularization, suggesting a broader impact on endothelial function. Previous studies have reported that globoidnan A exhibits pronounced antiproliferative effects in multiple cancer cell lines, including C6 (rat brain tumor), HeLa (human cervical carcinoma), and HT29 (human colon carcinoma) cells [30]. In the present context, the high predicted affinity of both malaxinic acid and globoidnan A for the NK-1 receptor indicates the need for further mechanistic studies to determine whether these interactions translate into functional modulation of neurogenic inflammation and tumor-associated signaling pathways.

Several limitations should be acknowledged. The present study focused exclusively on the A549 epithelial lung carcinoma cell line, and the inclusion of non-tumoral control cell lines, such as healthy fibroblasts or epithelial cells, would strengthen the interpretation of selectivity. Moreover, the observed inconsistencies in IL-6 and SP responses suggest that additional experimental validation, including expanded cytokine profiling and repeated ELISA measurements, is required. Finally, the *in silico* analyses were limited to molecular docking, and it should be emphasized that these results represent predictive interactions rather than direct evidence of biological activity; therefore, molecular dynamics simulations and in vivo studies are necessary to validate binding stability, receptor modulation, and pharmacological relevance.

5. CONCLUSION

Overall, the combined experimental and computational data support the hypothesis that phenolic constituents of *S. officinale* may exert anticancer effects through multi-target modulation of inflammatory and angiogenic pathways. These findings provide a rationale for further investigation into the extract's effects on cell viability, anti-inflammatory, and anti-angiogenic activities and highlight its potential as a promising source of therapeutic lead compounds.

CONFLICT OF INTEREST

The authors stated that there are no conflicts of interest regarding the publication of this article.

CRediT AUTHOR STATEMENT

Esra Tanyel Akçit: Software, Formal analysis, Investigation. **Nüket Akanıl Bingöl:** Conceptualization, Methodology. **Ece Şimşek:** Methodology, Validation, Writing – Review & Editing. **Altınay Altınkaynak:** Validation**,** Formal analysis, Writing – Original Draft. **Gizem Tutkun:** Data Curation, Visualization. **Zeynep Burcu Mekik:** Software. **Cemilenur Ataş:** Visualization **Nilüfer İmir:** Editing **İlker Çinbilgel:** Validation. **Kübra Yıldırım:** Methodology, **Emel Cengiz Kaynakcı:** Visualization. **Ahmet Yılmaz Çoban:** Supervision.

REFERENCES

[1] Demirtas I, Erenler R, Elmastas M, Goktasoglu A. Studies on the antioxidant potential of flavones of *Allium vineale* isolated from its water-soluble fraction. Food Chem 2013; 136: 34–40. doi: 10.1016/j.foodchem.2012.07.086.

[2] Le V, Dolganyuk V, Sukhikh A, Babich O, Ivanova S, Prosekov A, Dyshlyuk L. Phytochemical analysis of *Symphytum officinale* root culture extract. Appl Sci 2021; 11: 4478. https://doi.org/10.3390/app11104478.

[3] Turkish Plants Data Service (TR), 2024. Available at: http://194.27.225.161/yasin/tubives/index.php (Accessed 28 June 2024).

[4] Staiger C. Comfrey: A clinical overview. Phytother Res 2012; 26: 1441–8. https://doi.org/10.1002/ptr.4612.

[5] Zengin G, Sinan KI, Ak G, Angeloni S, Maggi F, Caprioli G, Kaplan A, Cakilcioğlu U, Akan H, Jugreet S, Mahomoodally M. Preliminary investigation on chemical composition and bioactivity of differently obtained extracts from *Symphytum aintabicum*. Biochem Syst Ecol 2021; 94: 104203. https://doi.org/10.1016/j.bse.2020.104203.

[6] Trifan A, Opitz S, Josuran R, Grubelnik A, Esslinger N, Peter S, Bräm S, Meier N, Wolfram E. Is comfrey root more than toxic pyrrolizidine alkaloids? Salvianolic acids among antioxidant polyphenols in comfrey (*Symphytum officinale* L.) roots. Food Chem Toxicol 2018; 112: 178–87. https://doi.org/10.1016/j.fct.2017.12.051.

[7] Moreira R, Pereira DM, Valentão P, Andrade PB. Pyrrolizidine alkaloids: Chemistry, pharmacology, toxicology and food safety. Int J Mol Sci 2018; 19: 1668. https://doi.org/10.3390/ijms19061668.

[8] Salehi B, Sharopov F, Boyunegmez Tumer T, Ozleyen A, Rodríguez-Pérez C, Ezzat S, Azzini E, Hosseinabadi T, Butnariu M, Sarac I, Bostan C et al. *Symphytum* species: a comprehensive review on chemical composition, food applications and phytopharmacology. Molecules. 2019; 24: 2472. https://doi.org/10.3390/molecules24122272.

[9] Kumar R, Kishore K. Onosma L.: a review of phytochemistry and ethnopharmacology. Pharmacogn Rev 2013; 7: 140–51. https://doi.org/10.4103/0973-7847.120513.

[10] Li Y, Yan B, He S. Advances and challenges in the treatment of lung cancer. Biomed Pharmacother 31; 169: 115891. doi: 10.1016/j.biopha.2023.115891.

[11] Ngaha TYS, Zhilenkova AV, Essogmo FE, Uchendu IK, Abah MO, Fossa LT, Sangadzhieva ZD, Sanikovich VD, Rusanov AS, Pirogova YN et al. Angiogenesis in Lung Cancer: Understanding the Roles of Growth Factors. Cancers. 2023; 15: 4648. https://doi.org/10.3390/cancers15184648.

[12] Wang Y, Yuan S, Ma J, Liu H, Huang L, Zhang F. Substance P is overexpressed in cervical squamous cell carcinoma and promoted proliferation and invasion of cervical cancer cells in vitro. Eur J Histochem 2023; 31: 3746. doi: 10.4081/ejh.2023.3746.

[13] Kim S, Chen J, Cheng T, Gindulyte A, He J, He S, Li Q, Shoemaker BA, Thiessen PA, Yu B, Zaslavsky L, Zhang J, Bolton EE. PubChem 2019 update: improved access to chemical data. Nucleic Acids Res 2021; 49: 388–95. https://doi.org/10.1093/nar/gkaa971.

[14] Oberlies NH, Kim NC, Brine DR, Collins BJ, Handy RW, Sparacino CM, Wani M, Wall ME. Analysis of herbal teas made from the leaves of comfrey (*Symphytum officinale*): reduction of N-oxides results in order of magnitude increases in the measurable concentration of pyrrolizidine alkaloids. Public Health Nutr 2004; 7: 919–24. https://doi.org/10.1079/phn2004624.

[15] Yakan S, Dağlıoğlu YK, Erdoğan KE, Sağlamtaş R, Gülçin İ. Efectos antioxidantes y de cicatrización de heridas de la consuelda (*Symphytum officinale*). Rev Cienf FCV-LUZ 2025; 35: 8. https://doi.org/10.52973/rcfcv-e35566.

[16] Sowa I, Paduch R, Strzemski M, Zielińska S, Rydzik-Strzemska E, Sawicki J, Kocjan R, Polkowski J, Matkowski A, Latalski M, Wójciak-Kosior M. Proliferative and antioxidant activity of *Symphytum officinale* root extract. Nat Prod Res. 2018; 32: 605–9. https://doi.org/10.1080/14786419.2017.1326492.

[17] Roman GP, Neagu E, Moroeanu V, Radu GL. Concentration of *Symphytum officinale* extracts with cytostatic activity by tangential flow ultrafiltration. Roum Biotechnol Lett 2008; 13: 4008–13.

[18] Ham S, Choi K, Lee Y, Lee Y, Yoon J, Kim S, Park YH, Lee DS. Inhibition of hepatocellular carcinoma cell growth by the extract of *Symphytum officinale* L. and the possible mechanisms for this inhibition. J Food Sci Nutr 1997; 2: 236–40.

[19] Seigner J, Junker-Samek M, Plaza A, D'Urso G, Masullo M, Piacente S, Holper-Schichl YM, de Martin RA. *Symphytum officinale* Root Extract Exerts Anti-inflammatory Properties by Affecting Two Distinct Steps of NF-κB Signaling. Front Pharmacol 2019; 26: 289. https://doi.org/10.3389/fphar.2019.00289.

[20] Huang L, Cai Y, Sun X, Liu Y, Zhao J. The neuropeptide substance P promotes the proliferation and invasion of glioma cells through the activation of the NF-κB pathway. Oncol Rep 2017; 38: 326–32. https://doi.org/10.3892/or.2017.5664.

[21] Lai JP, Douglas SD, Ho WZ. Human lymphocytes express substance P and its receptor neurokinin-1. J Neuroimmunol 2021; 356: 577610. https://doi.org/10.1016/j.jneuroim.2021.577610.

[22] Yamaguchi Y, Sasano T, Itoh T, Kondo S, Abe M. Substance P mediates inflammatory signaling via the NK1 receptor in human airway epithelial cells. Am J Respir Cell Mol Biol. 2009; 40: 543–52. https://doi.org/10.1165/rcmb.2008-0061OC.

[23] Chen L, Huang J, Ji H, Zhang X, Wang J. The role of substance P in inflammatory diseases. Mediat Inflamm 2015; 925860. https://doi.org/10.1155/2015/925860.

[24] Pagadala NS, Syed K, Tuszynski J. Software for molecular docking: a review. Biophys Rev 2017; 9: 91–102. https://doi.org/10.1007/s12551-016-0247-1.

[25] Salmaso V; Moro S. Bridging Molecular Docking to Molecular Dynamics in Exploring Ligand-Protein Recognition Process: An Overview. Front Pharmacol 2018; 9: 393738. https://doi.org/10.3389/fphar.2018.00923

[26] Gioia D, Bertazzo M, Recanatini M, Masetti M, Cavalli A. Dynamic Docking: A Paradigm Shift in Computational Drug Discovery. Molecules 2017; 22: 2029. https://doi.org/10.3390/molecules22112029.

[27] Singh H, Du J, Singh P, Yi T. Role of green silver nanoparticles synthesized from *Symphytum officinale* leaf extract in protection against UVB-induced photoaging. J Nanostruct Chem 2018; 8: 359–68. https://doi.org/10.1007/s40097-018-0281-6.

[28] Yang M, Gatot D, Mardia A. Efficacy of *Allium sativum*, *Curcuma longa* and *Zingiber officinale* extract on serum vasculoendothelial growth factors levels of breast cancer patients. Int J Res Rev 2021. https://doi.org/10.52403/ijrr.20211053.

[29] D'Urso G, Masullo M, Seigner J, Holper-Schichl YM, de Martin R, Plaza A, Piacente S. LC–ESI–FT–MS^n metabolite profiling of *Symphytum officinale* L. roots leads to isolation of comfrey A, an unusual arylnaphthalene lignan. Int J Mol Sci 2020; 21: 4671. https://doi.org/10.3390/ijms21134671.

[30] Erenler R, Yildiz I, Aydin A, Genc N. Antiproliferative and cytotoxic effects of bioactive compounds isolated from *Onosma bourgaei*. Med Oncol 2022; 39: 116. https://doi.org/10.1007/s12032-022-01705-z.